Turkish Journal of Electrical Engineering & Computer Sciences

http://journals.tubitak.gov.tr/elektrik/

Research Article

Turk J Elec Eng & Comp Sci
(2016) 24: 3293 – 3308

doi:10.3906/elk-1408-208

Thermal model of oil power transformers with a tap changer

Zoran RADAKOVIC[1,*], **Stefan TENBOHLEN**[2]
[1]School of Electrical Engineering, University of Belgrade, Belgrade, Serbia
[2]Institute of Power Transmission and High Voltage Technology (IEH), University of Stuttgart, Stuttgart, Germany

Received: 10.09.2014 • **Accepted/Published Online:** 04.04.2015 • **Final Version:** 15.04.2016

Abstract: The paper presents a new method for on-line temperature calculation taking into account change in the tap changer position. The method introduces accurate calculation of the losses, depending on the current, average temperature of the winding, and tap changer position (it affects both Joules (DC) losses and stray losses). The thermal model itself is the common three-body model (for a transformer with two windings per phase), with temperature dependent thermal conductances. Elements of the model describing steady-state characteristics are determined based on detailed construction and calculation of distribution of losses in the windings using the finite-elements method (FEM) and calculation of distribution of temperatures using the detailed thermal-hydraulic network model (THNM). Detailed calculation of the losses and temperatures enables the determination of the hot-spot factor ($H = Q\ S$); factor Q describes the nonuniform losses and factor S describes nonuniform cooling. The paper shows how these factors depend on tap changer position and the load.

Key words: Power transformer, losses, tap changer, loading, temperature

1. Introduction

The hot-spot insulation temperature represents typically the most important limiting factor for transformer loading [1]. The hot-spot temperature has to be under a prescribed limit value. A cumulative effect of insulation ageing, depending on the variation in hot-spot temperature in time, should be less than a planned value. Therefore, there is interest in knowing the hot-spot temperature at every moment of a real transformer operation, but also there is a need to predict its value if grid operators aim to overload transformers to a certain extent.

It is difficult to determine accurately the value of hot-spot temperature during transformer operation; on one side the transient thermal processes appearing during operation of the transformer are complicated and on the other side there is a strong need to have simple mathematical models for calculations running on-line. Another issue is the set of data needed for defining the parameters of the model. These data can be: a) results of calculation in the design phase, based on detailed construction, b) factory heat run tests results, and c) measurements during operation of the transformer. An example of parameterization of a thermal model based on data measured in heat run tests is presented in [2]. Reference [3] describes a model oriented to top oil temperature, requiring no data from the design stage and no data from heat run tests. Reference [4] deals with the change in parameters of a thermal model when the cooling system is controlled (number of compact coolers being changed) and due to pollution of the coolers. In this paper the model is based on detailed design data of

*Correspondence: radakovic@etf.rs

the transformer and the results of calculations using a detailed thermal-hydraulic network model (THNM) [5].

The three-body model used in this paper for the two-winding transformer is in line with the old IEC loading guide model [6] and model from [2]. The IEC loading guide [7] identifies the problem of hot-spot to top pocket oil overshoot and tries to solve it. Annex G of the IEEE loading guide [8] suggests a thermal model based on bottom oil; the issue of overshoot of temperature gradient hot spot to top oil by increase in load is also discussed in [9], where a model based on bottom oil is proposed.

The goal of this paper is to develop a procedure for accurate calculation of the losses (in particular at different tap changer positions), being the input data for the thermal calculation. In addition, the method offers improvement of the calculation of steady-state temperatures of each of the windings. For dynamic characteristics no improvement is made and transients are modeled according to state of the art methods.

2. Thermal circuit and difference equations

The dynamic thermal model is based on a thermal circuit with 3 nodes, presented in Figure 1.

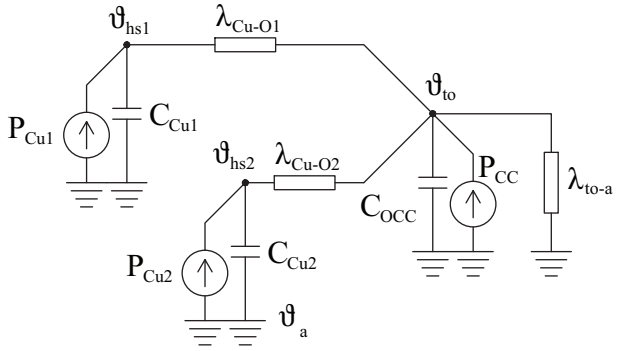

Figure 1. Nonlinear dynamic thermal circuit with 3 nodes

The mathematical model corresponds to the thermal circuit shown in Figure 1:

- Initial condition (time instant $k = 1$, t $= 0$):

$$\vartheta_{hs1}(t=0) = \vartheta^1_{hs1}, \vartheta_{hs2}(t=0) = \vartheta^1_{hs2}, \vartheta_{to}(t=0) = \vartheta^1_{to}$$

- Thermal conductances vary in time and they are calculated in every time instant k (t = (k - 1) Δt, Δt - calculation time step) using equations:

$$\lambda^k_{Cu-O1} = K_{hs1} \cdot \left(\vartheta^k_{hs1} - \vartheta^k_{to}\right)^{n_{hs1}} \tag{1}$$

$$\lambda^k_{Cu-O2} = K_{hs2} \cdot \left(\vartheta^k_{hs2} - \vartheta^k_{to}\right)^{n_{hs2}} \tag{2}$$

$$\lambda^k_{to-a} = K_{to} \cdot \left(\vartheta^k_{to} - \vartheta^k_{a}\right)^{n_{to}} \tag{3}$$

The dependences (1)–(3) are the same as those used in [2]. They can be improved by taking into account dependence of thermal conductance on absolute level of temperature in the transformer. Ambient temperature can be introduced into functional dependence, or at least two values of parameters K and n can be used: one for winter season and one for summer season. The idea for such improvement originates from the strong dependence of thermal viscosity on temperature, influencing convection heat transfer.

- Difference equations (time instant $k+1$):

$$\vartheta_{hs1}^{k+1} = \vartheta_{hs1}^{k} + \frac{\Delta t}{C_{Cu1}} \cdot (P_{Cu1}^{k} - \frac{C_{Cu1}}{\Delta t} \cdot \left(\vartheta_{a}^{k+1} - \vartheta_{a}^{k}\right) - (\vartheta_{hs1}^{k} - \vartheta_{to}^{k}) \cdot \lambda_{Cu-O1}^{k}) \tag{4}$$

$$\vartheta_{hs2}^{k+1} = \vartheta_{hs2}^{k} + \frac{\Delta t}{C_{Cu2}} \cdot (P_{Cu2}^{k} - \frac{C_{Cu2}}{\Delta t} \cdot \left(\vartheta_{a}^{k+1} - \vartheta_{a}^{k}\right) - (\vartheta_{hs2}^{k} - \vartheta_{to}^{k}) \cdot \lambda_{Cu-O2}^{k}) \tag{5}$$

$$\begin{aligned} \vartheta_{to}^{k+1} \quad = \quad & \vartheta_{to}^{k} + \tfrac{\Delta t}{C_{OCC}} \cdot \left(P_{CC}^{k} + (\vartheta_{hs1}^{k} - \vartheta_{to}^{k}) \cdot \lambda_{Cu-O1}^{k} + (\vartheta_{hs2}^{k} - \vartheta_{to}^{k}) \cdot \lambda_{Cu-O2}^{k}\right. \\ & \left. - \tfrac{C_{OCC}}{\Delta t} \cdot \left(\vartheta_{a}^{k+1} - \vartheta_{a}^{k}\right) - (\vartheta_{to}^{k} - \vartheta_{a}^{k}) \cdot \lambda_{to-a}^{k}\right) \end{aligned} \tag{6}$$

3. Distribution of losses in windings for different tap changer positions

The distribution of the magnetic field and consequent stray losses depend on the tap position. They can be calculated by custom-made software or some commercial finite elements programs (multi-physics or specialized for magnetic fields). Detailed geometry and size of the conductor and its strands are needed as input data for such high accuracy calculations. We performed such 2D calculations in two planes: in the central window plane and in the plane perpendicular to it (Figure 2); the figure presents the case of a transformer with LV and HV windings. From each of these calculations, four values of stray losses per volume unit for each of the conductors ($\mathrm{W/m^3}$) are calculated (p_{eI} – p_{eIV}). There is an essential difference in field distribution in the zone of core I and in other three zones (Figure 2). Considering the position of the winding, the average losses in each of conductors, in three phases, are equal to ($4\ p_{eI} + 2\ p_{eII} + 3\ p_{eIII} + 3\ p_{eIV}$)/12; multiplying this average value by the volume of the conductor give the losses in the conductor (P_e). DC losses in each of the conductors are calculated using the elementary product of resistance and squared conductor current: $P_{DCr}{=}\rho_{20}\frac{235+\vartheta_r}{235+20}\frac{l}{S}I_r^2$ where l is the circumference of the turn and S the cross-section of the conductor; ϑ_r represents conductor temperature; for copper $\rho_{20}{=}\ 1.68{\cdot}10^{-8}\Omega m$. Total losses at conductor temperature ϑ_r are equal to the sum of stray losses and DC losses: $P_{Totr}{=}P_{Sr}{+}P_{DCr}$. Eddy losses are proportional to the square of the current, but, contrary to DC losses, proportional to $1/\rho$.

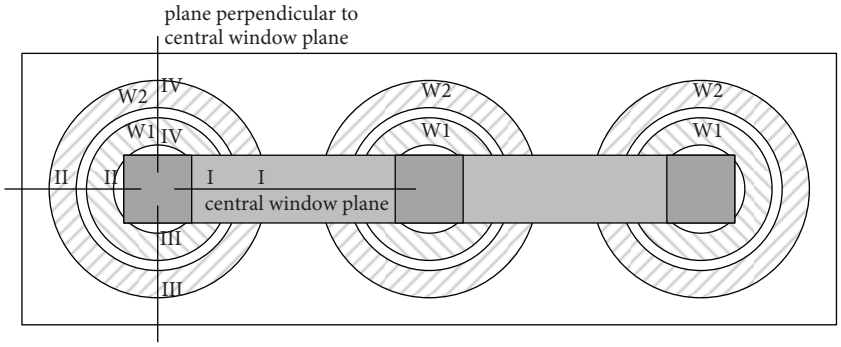

Figure 2. Boundaries for the calculation in two planes.

The above text relates to fixed topology of the conductors of the windings. When the tap position changes, some of conductors are connected/disconnected on the high voltage side and a new topology appears and causes change in field distribution and change in stray losses. Therefore, the calculation of losses by FEM calculations should be done for each tap position 'j'.

4. Determination of total losses in the winding in real operation

As discussed in the previous section, the losses in each conductor depend on the field at the position of conductor (depending on tap position), and on current and conductor temperature.

The temperature of winding conductors is not constant, and for very accurate calculation of power losses the temperature of each conductor should be known. Since the temperatures of conductors depend on the losses, an iterative procedure is to be applied. Such an option is of interest in thermal design, i.e. it can be implemented in software tools for thermal design of transformers [5].

In dynamic (on-line) thermal calculations, it is not realistic to calculate the temperature of each conductor and an estimation of power losses injected to the nodes of the thermal circuit (Figure 1) is done in the following way:

1. The stray and DC losses in each conductor are calculated for each of 'j' tap positions, by specified (same) temperature of all conductors (ϑ_r) and specified current I_r.

2. Total referent (at I_r and ϑ_r) DC losses ($P_{DCri}^{(j)}$) and stray losses ($P_{Sri}^{(j)}$) in each 'i' winding at each 'j' tap position are equal to the sum of the losses in each conductor calculated for winding 'i' by tap position 'j' and for referent current I_r and referent temperature ϑ_r.

3. The total losses in each 'i' winding at each 'j' tap position ($P_{Wi}^{(j)}$) in real operating conditions are calculated supposing uniform temperature over the winding, being equal to average winding temperature (ϑ_{Wai}); determination of this temperature in each moment of transformer operation is discussed in the next section. The losses in each of the windings at current I are calculated as

$$P_{Wi}^{(j)} = P_{DCri}^{(j)} \frac{235+\vartheta_{Wai}}{235+\vartheta_r} \left(\frac{I}{I_r}\right)^2 + P_{Sri}^{(j)} \frac{235+\vartheta_r}{235+\vartheta_{Wai}} \left(\frac{I}{I_r}\right)^2 \tag{7}$$

5. Determination of cooling hot-spot factor S

Nonuniformity of conductor temperature over the winding originates from nonuniform losses (described with factor Q), but also from nonuniform cooling (factor S) [10,11]. Namely, the oil flow in cooling ducts is not uniform, causing variable oil temperatures and convection heat transfer coefficients. The thickness of the insulation of conductors in some cases changes, causing nonuniform thermal resistance to heat conduction. The influence of nonuniform cooling is described with factor S.

Factor Q can be determined from results of FEM calculations of the losses at referent current I_r and referent temperature ϑ_r. This factor for each of the windings ($Q_i^{(j)}$) is equal to the ratio of the losses in the conductor with the highest losses and average value of the losses in all conductors.

Theoretically, the cooling hot-spot factor (S) depends on tap position (distribution of oil velocity theoretically depends on distribution of losses), but it is a "second order effect", which can be neglected. Accordingly, the cooling hot-spot factor was calculated only for one tap position (zero position, $j = 8$), but for more load levels (60%, 70%, 80%, 85%, 90%, 95%, and 100% of rated load); as shown in Figures 3 and 4, the cooling hot-spot factor changes with load. The procedure, applied to each of the windings 'i' and each of the load levels 'k', for specified ambient temperature ϑ_a, is as follows:

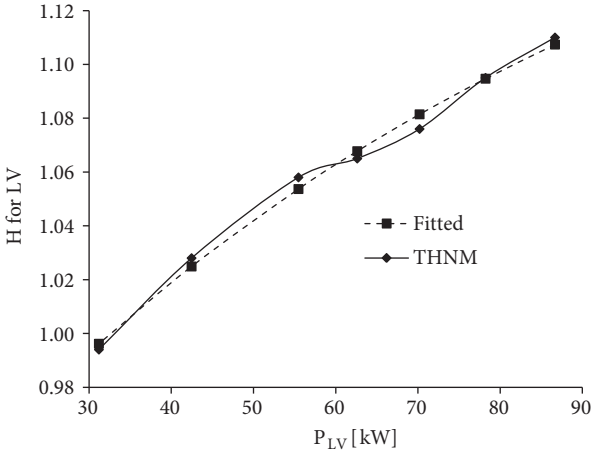

Figure 3. H factor for LV winding.

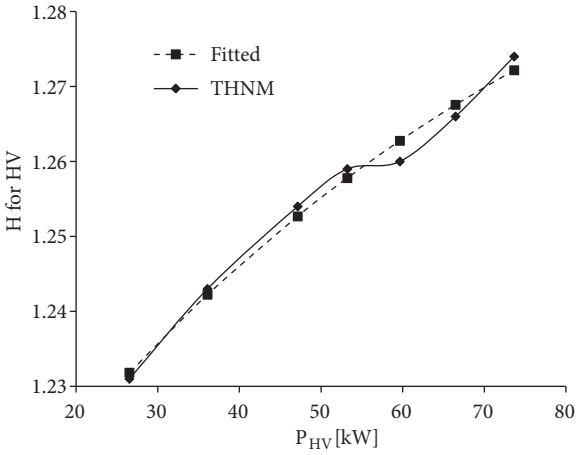

Figure 4. H factor for HV winding.

1. The thermal calculation of a complete transformer using software based on a detailed THNM, with data about losses in each conductor obtained from the FEM, is performed. The results of the calculation are all characteristic quantities: total hot-spot factor (H_{ik}), average winding to average oil temperature gradients (θ_{WaOaik}), vertical oil gradients in the windings (θ_{OWik}) and in the cooler (θ_{OCk}) and oil at the bottom of the windings (ϑ_{ObWik}) and at the bottom of the cooler (ϑ_{ObCk}).

2. Cooling hot-spot factor (S_{ik}) is calculated from H_{ik} and losses hot-spot factor, determined from once calculated distribution of power losses ($Q_i^{(j=8)}$): $S_{ik} = H_{ik} / Q_{ik}$

6. Determination of parameters of thermal network

Coefficients of thermal conductances K_{hs1}, n_{hs1}, K_{hs2}, n_{hs2}, K_{to}, and n_{to} (Eqs. (1)–(3)) are determined using results of software for thermal calculations based on the detailed THNM for the above specified loads of 60%, 70%, 80%, 85%, 90%, 95%, and 100% of rated load. Since there are two parameters in function (1)–(3) for each of the thermal conductances, these two parameters can theoretically be determined from the values of the losses and calculated temperature differences in two steady states ((1) and (2)) as (example for K_{to} and n_{to}):

$$n_{to} = \frac{\ln \frac{P_{Cu1(1)}+P_{Cu2(1)}+P_{CC(1)}}{P_{Cu1(2)}+P_{Cu2(2)}+P_{CC(2)}}}{\ln \frac{(\vartheta_{to}-\vartheta_a)_{(1)}}{(\vartheta_{to}-\vartheta_a)_{(2)}}} - 1 \tag{8}$$

$$K_{to} = \frac{P_{Cu1(1)} + P_{Cu2(1)} + P_{CC(1)}}{(\vartheta_{to} - \vartheta_a)_{(1)}^{n_{to}+1}} \tag{9}$$

Nevertheless, due to sensitive logarithmic function and small imprecision of calculation, the pairs of n and K parameters should be determined from temperatures calculated for more than two loads [12]; the results of the application of the procedure are presented in Section 10.3.

Thermal capacitances of the windings are more difficult to determine. As explained in [2], it can be done from the recording of the average winding temperature during transient thermal processes, applying a numerical method for parameter estimation.

If such measurement data are not available, a simplified method has to be applied. An option is to calculate it as the sum of products of the mass and specific heat of material, where nonuniform distribution of temperature over the parts should be considered.

The capacitances used in simulations of dynamic thermal processes in Section 10 are determined by multiplying the time constant by thermal conductance (at rated load and rated temperature rises). Typical values for thermal time constants (5 min for the winding, $\tau_{Cu} = 5$ min, and 3 h for node representing oil, core and tank, $\tau_{OCC} = 3$ h) are assumed. Accordingly,

$$C_{Cu1} = K_{hs1} \cdot (\vartheta_{hsr1} - \vartheta_{tor})^{n_{hs1}} \cdot \tau_{Cu} \tag{10}$$

$$C_{Cu2} = K_{hs2} \cdot (\vartheta_{hsr2} - \vartheta_{tor})^{n_{hs2}} \cdot \tau_{Cu} \tag{11}$$

$$C_{OCC} = K_{to} \cdot (\vartheta_{tor} - \vartheta_a)^{n_{to}} \cdot \tau_{OCC} \tag{12}$$

If data about the change of top oil temperature during a transient thermal process are available, thermal capacitances can be determined using a numerical estimation method [2,12]. The most realistic case is that only measurements of top oil are available (no special measurements during heat run test such as described in [2] nor fiber optics measurements of winding temperature). In this case, the thermal capacity of oil, core, and tank (C_{OCC}) can be determined accurately and the thermal capacitance of the windings approximately (Eqs. (10) and (11)). Since change in top oil temperature is much slower than the change in windings to oil temperature difference, the approximation for the winding thermal capacitance does not cause a calculation error in oil temperature.

7. Complete methodology for dynamic temperature calculation

Hot spot temperature of each of the windings and top oil temperature are calculated according to the thermal circuit in Figure 1 (corresponding Eqs. (4)–(6) are used to calculate temperatures at every discrete moment of transformer operation ($k\ \Delta t$; $k = 1, 2, 3, ...$) starting from the initial state ($t = 0$) with known temperatures).

Change in ambient temperature in time is the input data.

The losses are calculated also at every calculation step, based on input data of current load (I), tap changer position (j), and on average winding temperature in the previous calculation step (($k - 1$) Δt), according to Eq. (7). Average winding temperature used for the calculation of the losses is calculated as

$$\vartheta^k_{Cua1} = \frac{\vartheta^k_{hs1} - \vartheta^k_{to}}{S^k_1 Q^{k(j)}_1} + \left(\vartheta^k_{to} - 0.5\theta^k_{OC}\right) \tag{13}$$

$$\vartheta^k_{Cua2} = \frac{\vartheta^k_{hs2} - \vartheta^k_{to}}{S^k_2 \cdot Q^{k(j)}_2} + \left(\vartheta^k_{to} - 0.5\theta^k_{OC}\right) \tag{14}$$

Comments on Eqs. (13) and (14):

1. As discussed in Section 4, cooling hot-spot factor (S^k_i) is taken to be independent on tap changer position, while the losses hot-spot factor depends on tap position ($Q^{k(j)}_1$, $Q^{k(j)}_2$), which can vary in time due to change in tap position (j) in time.

2. As will be shown in Chapter 10.3., calculations using the detailed THNM yield the result that cooling hot-spot factor (S_i^k) changes with the change in current load; losses hot-spot factor does not depend on the current load. At this point slight approximation has been made that S_i depends only on load level, i.e. it is considered that it does not change during transient thermal processes.

3. The second term in Eqs. (13) and (14) $\left(\vartheta_{to}^k - 0.5\theta_{OC}^k\right)$ is the average oil temperature in calculation step k. It is obtained by subtracting half of vertical oil temperature gradient from top oil temperature. Functional dependence of θ_{OC} on total losses is obtained from the detailed THNM for different values of losses in steady states ($\vartheta_{OC} = f(P_{Tot})$); the value of vertical temperature gradient in on-line calculations is determined from this functional dependence, where the losses are equal to power transferred from oil to ambient; they are calculated using the thermal circuit from Figure 1 ($P_{Tot} = P_{O-a} = (\vartheta_{to}^k - \vartheta_a^k) \cdot \lambda_{to-a}^k$).

The losses in a common node are calculated as the sum of constant value of core losses (equal to the rated core losses) and the losses in the tank and constructive parts. The second component is calculated as the product of square of per unit current load at the LV side and the losses in the tank and constructive parts by rated current, determined using the results of the factory acceptance tests.

8. Brief description of the case-study ONAF transformer 40 MVA

A three phase transformer with high voltage, low voltage, and tertiary windings, YNyn0 + d1, 132 / 13.8 / 11 kV, rated power in ONAF mode 40 / 40 / 13.33 MVA, with 2 cooling blocks mounted on tank, each with 4 radiators, each radiator with 29 plates of height 1.9 m is under investigation. There are five windings: tertiary (TV), low voltage (LV) and high voltage being assembled from main winding (HV_ M) and two regulating windings (HV_ C and HV_ F); regulating range –12 × 1.43% to + 7 × 1.43% = –15.73% to +10%. Constructions of the windings are: TV - layer winding cooled only on inner and outer axial cooling ducts, LV - zig-zag cooled layer winding (9 passes, 11 or 12 radial duct per pass, only one CTC conductor in radial direction), HV_ M - zig-zag cooled disc winding (10 passes, 9 to 11 radial duct per pass, 18 conductors in radial direction), HV_ C - layer winding cooled only on inner and outer axial cooling duct and HV_ F - layer winding cooled only on inner and outer axial cooling duct. Total losses in all windings at the tap position corresponding to rated voltage ("zero position") are 167.4 kW, losses in main windings: LV - 28889 W per phase and in HV_ M - 24552 W per phase.

9. Results of calculations of investigated transformer

9.1. FEM calculation of distribution of winding losses for different tap positions

Tables 1 (for LV winding) and 2 (for HV_ M winding) present the results of simple postprocessing of FEM calculation results; electrical hot-spot factor Q presents the ratio of the losses in the conductor with the highest losses and the average value of the losses in all conductors. The values in Tables 1 and 2 are given for current in LV winding equal to rated current and uniform temperature of conductors over the windings, being equal to 75 °C. Tap position 1 is the position with maximum voltage (145.213 kV) and tap position 20 with minimum voltage (109.342 kV). Tap position 8 is "zero position", corresponding to rated voltage.

Table 1. Data obtained for LV winding using the FEM (by fixed rated current of LV side and uniform temperature of 75 °C).

Tap position	LV			
	DC losses (W)	Eddy losses (W)	Total losses (W)	Factor Q
1	28,351.5	546.6	28,898.1	1.026
2	28,351.5	548.9	28,900.3	1.027
3	28,351.5	549.7	28,901.3	1.027
4	28,351.5	550.1	28,901.7	1.027
5	28,351.5	549.6	28,901.2	1.027
6	28,351.5	548.8	28,900.3	1.028
7	28,351.5	548.0	28,899.6	1.028
8	28,351.5	537.6	28,889	1.024
9	28,351.5	538.7	28,890.2	1.023
10	28,351.5	552.4	28,903.9	1.027
11	28,351.5	539.5	28,891.0	1.023
12	28,351.5	553.1	28,904.6	1.027
13	28,351.5	555.2	28,906.7	1.027
14	28,351.5	545.8	28,897.3	1.023
15	28,351.5	556.0	28,907.5	1.028
16	28,351.5	555.3	28,906.8	1.028
17	28,351.5	543.8	28,895.3	1.024
18	28,351.5	542.4	28,893.9	1.024
19	28,351.5	553.8	28,905.4	1.027
20	28,351.5	555.8	28,907.3	1.026

Table 2. Data obtained for main HV winding using the FEM (by fixed rated current of LV side and uniform temperature of 75 °C).

Tap position	HV_ M			
	DC losses (W)	Eddy losses (W)	Total losses (W)	Factor Q
1	18,963.1	1759.6	20,722.7	1.332
2	19,454.7	1760.7	21,215.4	1.321
3	19,971.9	1700.5	21,672.4	1.295
4	20,515.7	1727.9	22,243.6	1.314
5	21,086.7	1707.1	22,793.8	1.314
6	21,685.8	1686.1	23,371.8	1.318
7	22,313.8	1657.1	23,970.9	1.323
8	22,971.6	1580.3	24,552	1.310
9	23,660.1	1552.9	25,213.0	1.315
10	24,380.2	1525.3	25,905.5	1.319
11	25,132.9	1498.0	26,630.9	1.313
12	25,919.2	1498.3	27,417.5	1.301
13	26,740.1	1490.3	28,230.4	1.296
14	27,596.6	1478.8	29,075.4	1.295
15	28,489.8	1464.5	29,954.3	1.296
16	29,420.8	1445.7	30,866.5	1.298
17	30,390.7	1402.5	31,793.2	1.298
18	31,400.7	1395.3	32,796.0	1.306
19	32,452.0	1413.2	33,865	1.327
20	33,545.8	1349.1	34,894.9	1.314

The DC losses in LV do not change since the current and temperature are fixed and the number of conductors does not change. The DC losses in HV_ M (main HV windings) change since the current changes due to change in the windings turn ratio. As expected, the eddy losses in inner LV winding stay almost constant, while the eddy losses in HV_ M change, but not much. More intensive change in eddy losses appears in regulating HV windings, as presented in Table 3. Since only the temperature of main windings (LV and HV_ M) is calculated in variable loading conditions, the losses in HV_ C and HV_ F windings are added to the common node (added to core losses and losses in tank and constructive parts). Multiplication of square per unit current is done, while dependence on temperature is neglected.

Table 3. DC and eddy losses in regulating HV windings using the FEM (by fixed rated current of LV side and uniform temperature of 75 °C).

Tap position	HV_ C		HV_ F	
	DC losses (W)	Eddy losses (W)	DC losses (W)	Eddy losses (W)
1	4174.0	242.6	4120.5	134.4
2	4282.2	214.3	3757.6	157.8
3	4396.0	187.9	3375.3	169.9
4	4515.7	148.8	2971.9	197.2
5	4641.4	116.4	2545.5	219.4
6	4773.3	84.74	2094.3	243.5
7	4911.5	56.86	1616.2	269.2
8	5056.3	34.6	1109.2	287.6
9	5207.8	21.9	571.2	316.5
10	5366.3	30.16	0	352.2
11	0	96.1	5461.2	48.0
12	0	87.7	5006.2	64.2
13	0	82.7	4519.2	76.7
14	0	80.7	3997.7	90.0
15	0	82.7	3439.2	105.0
16	0	90.2	2841.3	121.5
17	0	101.3	2201.2	136.4
18	0	129.9	1516.2	159.1
19	0	176.3	783.5	187.6
20	0	233.0	0	207.6

9.2. THNM calculation of steady states in different loading conditions

The calculations are done for series of current loads: 60%, 70%, 80%, 85%, 90%, 95%, and 100% of rated current on the LV side.

The calculations are done for tap position 8 (corresponding to rated voltage). The temperature is fixed at 75 °C when calculating power losses in the winding; it mean the losses amounted to: 36%, 49%, 64%, 72.25%, 81%, 90.25%, and 100% of the losses by rated current of the LV side and fixed tap position 8.

Table 4 presents results for ambient temperature $\vartheta_a = 25.3$ °C and the above specified load. The losses in node corresponding to oil, core, and tank are equal to the sum of losses in tertiary winding, two HV regulating windings (the dependence of these losses on current load is taken into account; losses by rated current amount 57.6 W, 5091 W, and 1397 W, respectively) and the losses in tank and in constructive parts inside the tank. Measured losses in tap position 8 in short-circuit by rated current, recalculated to 75 °C, are 194.28 kW,

meaning that the losses in the tank and constructive part are equal to 194,280 – 3 (57.6 + 28,889.1 + 24,551.9 + 5091 + 1397) = 14,320 W. They are divided roughly as: 4.32 kW in tank surfaces and 2 × 5 kW = 10 kW in constructive parts; this distribution of losses can be estimated roughly since it does not influence significantly the final distribution of the temperature. It is assumed that there are no losses in the core, since the heat run test in short-circuit is considered. For all components it is assumed that they are proportional to the per unit current load.

Table 4. Results of calculations using detailed THNM

Current load	%	100	95	90	85	80	70	60
Total losses	kW	194.3	175.3	157.4	140.4	124.3	95.20	69.94
Losses in LV node	kW	86.7	78.22	70.20	62.62	55.47	42.47	31.20
Losses in HV node	kW	73.7	66.47	59.66	53.22	47.14	36.09	26.52
Losses in oil, core and tank node	kW	34.0	30.64	27.50	24.53	21.73	16.64	12.22
$(\vartheta_{to} - \vartheta_a)$	K	35.8	33.60	31.43	29.29	26.81	23.26	19.21
$(\vartheta_{ao} - \vartheta_a)$	K	21.6	19.94	18.33	16.77	15.13	12.65	10.19
$\theta_{OC} = \vartheta_{to} - \vartheta_{bo}$	K	28.4	27.60	26.47	25.03	23.36	21.22	18.03
$(\vartheta_{Cua} - \vartheta_{ao})_{LV}$	K	15.4	14.23	13.05	11.86	10.76	8.72	6.89
$(\vartheta_{Cua} - \vartheta_{ao})_{HV}$	K	8.5	7.71	6.93	6.15	5.43	4.19	3.13
$(\vartheta_{Cuhs} - \vartheta_{to})_{LV}$	K	19.7	18.01	16.45	14.94	13.50	10.84	8.49
$(\vartheta_{Cuhs} - \vartheta_{to})_{HV}$	K	9.46	8.44	7.45	6.55	5.74	4.30	3.11
H_{LV}		1.274	1.266	1.260	1.259	1.254	1.243	1.231
H_{HV}		1.110	1.095	1.076	1.065	1.058	1.028	0.994
Total oil flow	m^3/h	10.294	9.671	9.075	8.471	8.07	6.845	5.975

H – hot-spot factor, calculated as $(\vartheta_{Cuhs} - \vartheta_{to})$ / $(\vartheta_{Cua} - \vartheta_{ao})$

Indexing key:

a - ambient

ao - average temperature of oil in the cooler, *to* - temperature of oil entering the cooler

Cu a - average winding temperature, *Cu hs* - hot-spot winding temperature

LV - low voltage winding, *HV* - high voltage winding

9.3. Parameters of thermal circuit with three nodes

It can be noted from Table 4 that hot-spot factor slightly changes with the change in load. Figures 3 (for LV winding) and 4 (for HV winding) show change in hot-spot factor (H), where the losses on the x axis are the losses in the winding; this change in hot-spot factor is a consequence of change in cooling hot-spot factor S, since values of losses hot-spot factors are constant for fixed tap position ($Q_{LV} = 1.024$ and $Q_{HV} = 1.310$ for tap position 8, see Tables 1 and 2).

The change in hot-spot factor with the load is fitted by functions

$$H_{LV} = 1.2318 + 0.08506\left(1 - e^{-\frac{(P_{LV}-31.2)/31.2}{2.7642}}\right) \tag{15}$$

$$H_{HV} = 0.99618 + 0.2340\left(1 - e^{-\frac{(P_{HV}-26.52)/26.52}{2.7575}}\right), \tag{16}$$

where P_{LV} and P_{HV} are winding power losses in all three LVs, i.e. HV windings, in kW.

Figure 5 shows dependence of LV hot spot minus top pocket oil temperature difference on LV winding losses; Figure 6 shows the same dependence for HV winding. Figure 7 shows the dependence of top pocket oil minus ambient temperature on total losses.

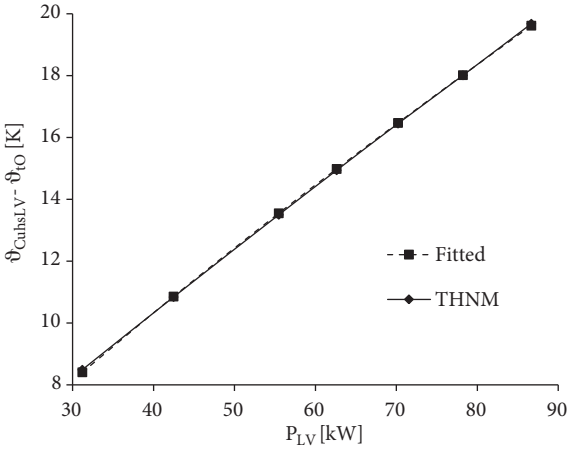

Figure 5. LV hot-spot minus top pocket oil temperature difference.

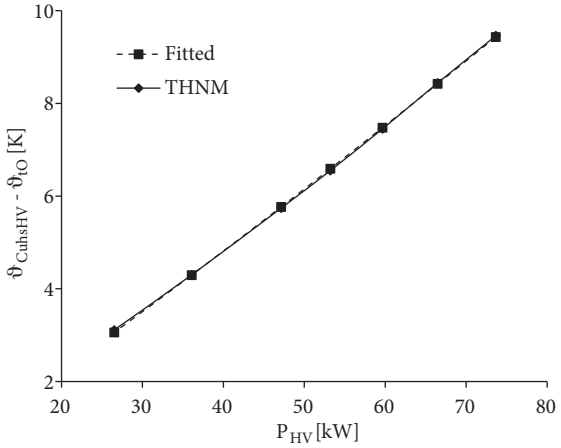

Figure 6. HV hot-spot minus top pocket oil temperature difference.

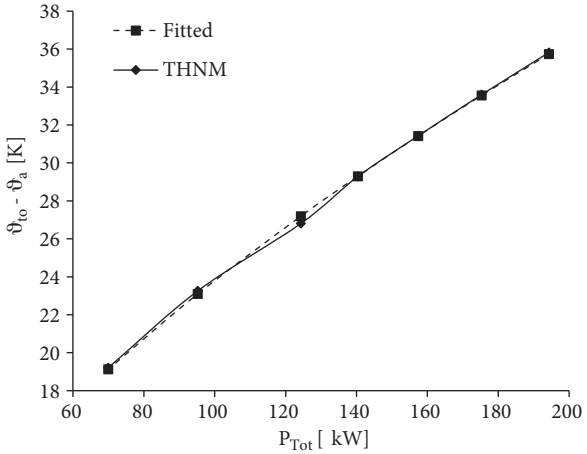

Figure 7. Top pocket oil minus ambient temperature rise.

The fitted functional dependences in Figures 5–7 are

$$\vartheta_{CuhsLV} - \vartheta_{to} = 0.484758 P_{LV}^{0.8293} \tag{17}$$

$$\vartheta_{CuhsHV} - \vartheta_{to} = 0.0824 P_{HV}^{1.1025} \tag{18}$$

$$\vartheta_{to} - \vartheta_{a} = 2.946 P_{Tot}^{0.4972} \tag{19}$$

The functions for average winding to average oil temperature differences, and for vertical oil temperature gradient in the radiators, obtained in the same manner as Eqs. (17)–(19), are

$$\vartheta_{CuaLV} - \vartheta_{ao} = 0.4402 P_{LV}^{0.79699} \tag{20}$$

$$\vartheta_{CuaHV} - \vartheta_{ao} = 0.11955 P_{HV}^{0.99223} \tag{21}$$

$$\vartheta_{to} - \vartheta_{bo} = 3.28 P_{Tot}^{0.41} \tag{22}$$

From Eqs. (17)–(19) we easily get the functional dependence of thermal conductances of thermal network from Figure 1–Eqs. (1)–(3):

$$\lambda_{Cu-O1} = 2.394 \cdot (\vartheta_{hs1} - \vartheta_{to})^{0.2058} \tag{23}$$

$$\lambda_{Cu-O2} = 9.6222 \cdot (\vartheta_{hs2} - \vartheta_{to})^{-0.09297} \tag{24}$$

$$\lambda_{to-a} = 0.5626 \cdot (\vartheta_{to} - \vartheta_{a})^{0.6343} \tag{25}$$

The thermal characteristics at rated conditions (using Eqs. (17)–(22)) are

$$(\vartheta_{CuhsLV} - \vartheta_{to})_r = 19.62$$

$$(\vartheta_{CuhsHV} - \vartheta_{to})_r = 9.43$$

$$(\vartheta_{CuaLV} - \vartheta_{ao})_r = 15.42$$

$$(\vartheta_{CuaHV} - \vartheta_{ao})_r = 8.52$$

$$(\vartheta_{to} - \vartheta_{a})_r = 40.27$$

$$(\vartheta_{to} - \vartheta_{bo})_r = 30.82$$

$$H_{LVr} = \frac{(\vartheta_{CuhsLV} - \vartheta_{to})_r}{(\vartheta_{CuaLV} - \vartheta_{ao})_r} = 1.272$$

$$H_{HVr} = \frac{(\vartheta_{CuhsHV} - \vartheta_{to})_r}{(\vartheta_{CuaHV} - \vartheta_{ao})_r} = 1.107$$

All characteristic winding to oil temperature differences and hot-spot factors are determined for conditions of rated current: total losses in all three LV windings are 86.67 kW and total losses in all three HV windings are 73.66 kW.

Both oil temperature rises are determined using the value of the total losses in the transformer under normal rated conditions of 236.14 kW.

9.4. Comparison of results obtained using detailed THNM and heat run test

The standard heat test according to IEC Standard [10] was performed for the case study transformer, with tap changer at position 19. The results of the heat run test and calculations obtained by the detailed THNM are presented in Table 5. Please note that the winding to oil temperature gradients are calculated for the steady state with rated current (for tap position 19 it amounts 207.6 A at the HV side), which does not fully correspond to conditions in real heat run test; oil temperatures are different since oil temperatures do not reach steady state after switching from total rated power losses to rated current.

Total rated losses applied in the first part of the heat run test were equal to the sum of rated load losses, rated core losses, and estimated solar radiation, amounting to 236.14 kW. The calculated DC and stray losses

in the windings at tap position 19 and rated current and temperature 75 °C amount to 191.9 kW. Measured losses in tap position 19 in short-circuit by rated current, recalculated to 75 °C, are 201.2 kW, meaning that the losses in the tank and constructive part are equal to 201191 W – 191926 W = 9265 W. These losses are divided as 2795 W in the tank and 6470 W in the construction parts in the tank (the distribution of the components is kept the same as adopted for tap position 8). In order to reach the specified total losses of 236.14 kW the current is increased in respect to rated for $\sqrt{\frac{236140W}{201191W}} = 1.0834$.

Table 5. Comparison of calculated values of temperatures rises (in respect to ambient) with the results of standard heat run test (tap position 19, ambient temperature 25.3 °C).

	Oil temperature rise (K)/total rated losses		Winding temperature rise (LV/HV)/rated current
	Top oil	Average oil	Average winding to average oil rise (K)
Heat run test	43.7	26.6	15.0 / 12.4
Calculated	42.9	26.7	13.9 / 13.4

10. Simulation of operation

10.1. General and load test pattern

The considered transformer is newly built and there are still no data from the field. That is why as a final result the paper offers the results of simulation, i.e. the change in hot-spot temperatures and top pocket oil temperature at supposed load profile. The pattern of input data is given in Table 6. The change in tap is not realistic, i.e. such change in tap position does not appear in real operations; such an unreal change was defined to highlight the influence of tap change. Initial state was a cold transformer, i.e. the temperature inside the transformer was equal to ambient temperature.

Table 6. Simulated theoretical load pattern.

Time (h)	Per unit current at LV side	Ambient temperature (°C)	Tap position
0	1	16	1
2	0.5	15	8
6	0.5	15	20
10	0.65	17	9
14	1.1	21	1
15	1	23	1
18	0.8	22	5
19	0.7	21	6
20	0.6	20	3
22	0.65	17	2
23	0.6	16	14
24	0.6	16	14

10.2. Calculation of the losses

The determination of the losses in the windings corresponding to nodes 1 and 2 of the thermal circuit in Figure 1 is described in detail in Section 4. Loss in the common node is calculated as the sum of constant value 19.2 kW (the rated core losses, obtained from factory tests); the losses in TV, HV_ C, and HV_ F windings; and the losses in tank and constructive parts due to stray flux, taken to be proportional to the square of per unit current

load at the LV side. The losses in the tank and constructive parts are calculated as follows. Starting points were the values of measured short-circuit losses in 3 tap positions: Tap 1, Tap 8, and Tap 19. Subtracting the losses in the windings calculated by FEM, the losses in the tank and constructive parts are calculated at these three tap positions (see Table 7). For other tap positions, the losses in the tank and constructive parts are interpolated using these three points. Example: for tap position 5, these losses at rated current are equal to

$$21.978 + ((5-1)/(8-1))(14.32 - 21.978) = 17.602kW.$$

Table 7. The losses (kW) at different tap positions at rated current * Measured in short-circuit at rated current, recalculated to 75 °C** Calculated at rated current, at 75 °C.

Tap position	1	8	19
Measured losses*	197.028	194.28	201.191
Winding losses**	175.05	179.96	191.926
Losses in tank and constructive parts	21.978	14.32	9.265

10.3. Results

The results of the simulation for the load pattern according to Table 6, the thermal circuit presented in Figure 1, and the parameters of the circuit specified by Eqs. (23)–(25) and (10)–(12), are presented in Figure 8.

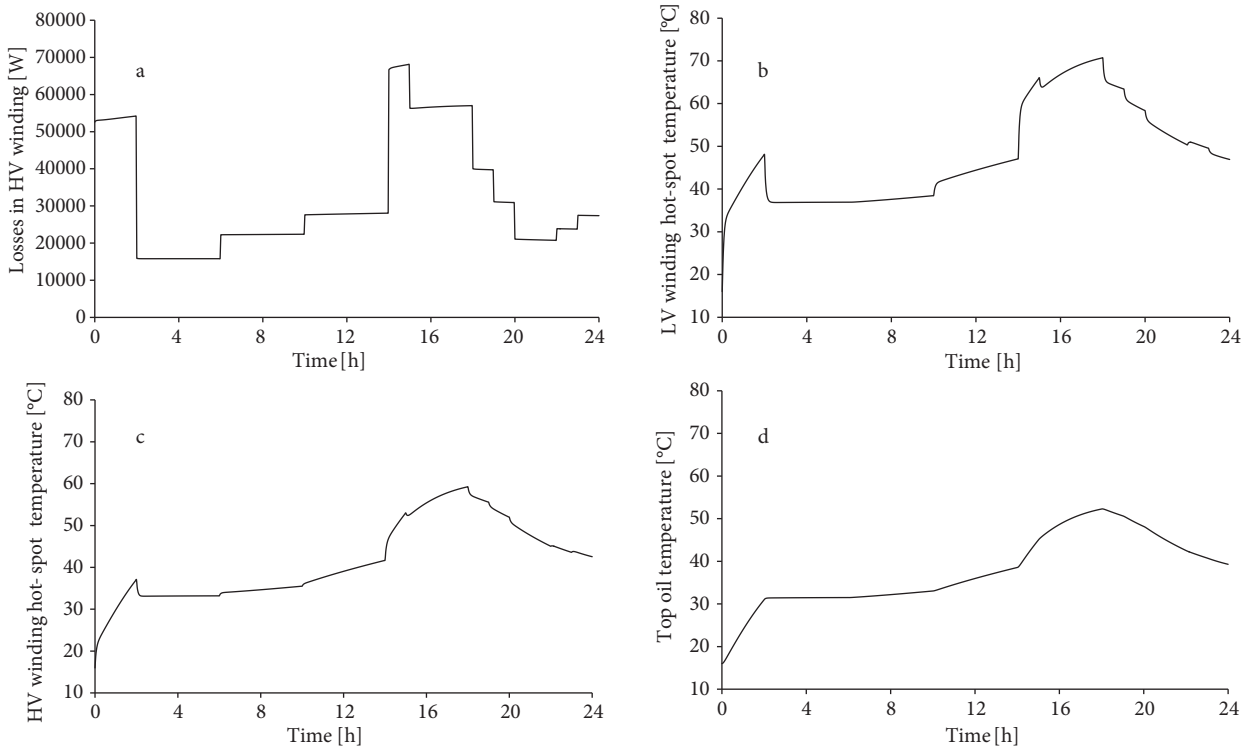

Figure 8. Results of simulation for pattern load from Table 6.

11. Plans for testing

This paper introduced a model that is at many points based on results of detailed calculation of the transformer using a detailed THNM. In addition to such a fundamentally new approach, the paper offers methodology for

calculation of losses considering each of their components and relevant influences. The natural planned step is testing of the model on representative records of data in real operations (one-year measurements seem to be representative). Since the focus of this paper is a thermal model for top oil, the set of data from operation should contain ambient temperature, tap position, load, and top pocket oil temperature.

12. Conclusions

The paper presents a method for the calculation of characteristic temperatures (hot spot temperature of each winding and top pocket oil temperature) under conditions of variable loading, ambient temperature, and tap changer position during the operation of oil immersed power transformers. The main enhancement of the described model is the method for the calculation of losses at different tap changer positions, considering all relevant elements (the method from valid IEC standard [7] is simplified).

The presented method for the calculation is based on FEM software for the losses and detailed THNM software for thermal characteristics. Performing these powerful tools enables determining functional dependences of hot-spot factors (total (H), losses (Q), and cooling (S)) and steady-state thermal characteristics (for example, of exponents x and y); the paper presents details of calculating winding hot-spot and top oil temperatures, but also temperature gradients and temperatures needed for accurate calculation of winding losses.

The methodology is applied to a transformer with a rated power of 40 MVA, for which details of constructions were known and heat run test data are available. It is planned to collect representative one-year measurements from the real operation of the transformer and to compare the measured values with the results obtained by the method presented in this paper.

Acknowledgment

The authors wish to express gratitude to the Alexander von Humboldt Foundation for support of this research.

References

[1] Georgilakis PS. Spotlight on Modern Transformer Design. London, UK: Springer, 2009.

[2] Radakovic Z, Kalic D. Results of a novel algorithm for the calculation of the characteristic temperatures in power oil transformers. Electr Eng 1997; 80: 205-214.

[3] Schmidt N, Tenbohlen S, Skrzypek R, Dolata B. Assessment of overload capabilities of power transformers by thermal modelling. In: CIGRE SC A2 and D1 Joint Colloquium 2011; 11–16 September 2011; Kyoto, Japan: PS1-O-28.

[4] Radakovic Z, Jacic D, Lukic J, Milosavljevic S. Loading of transformers in conditions of controlled cooling system. Int T Electr Energy 2014; 24: 203-214.

[5] Radakovic Z, Sorgic M. Basics of detailed thermal-hydraulic model for thermal design of oil power transformers. IEEE T Power Deliver 2010; 25: 790-802.

[6] IEC. IEC Publication 600354, Loading Guide for Oil-Immersed Power Transformers. Geneva, Switzerland: IEC, 1991.

[7] IEC. IEC Publication 60076-7, Loading Guide for Oil-Immersed Power Transformers. Geneva, Switzerland: IEC, 2005.

[8] IEEE. IEEE Standard C57.91-1995, IEEE Guide for Loading Mineral-Oil-Immersed Transformers. New York, NY, USA: IEEE, 1996.

[9] Radakovic Z, Feser K. A new method for the calculation of the hot-spot temperature in power transformers with ONAN cooling. IEEE T Power Deliver 2003; 18: 1284-1292.

[10] IEC. IEC Publication 60076-2 ed.3.0, Power Transformers - Part 2: Temperature Rise for Liquid-Immersed Transformers. Geneva, Switzerland: IEC, 2011.

[11] Radakovic Z, Radoman U, Kostic P. Decomposition of the hot-spot factor. IEEE T Power Deliver 2015; 30: 403-411.

[12] Radakovic Z. Numerical determination of characteristic temperatures in directly loaded power oil transformer. Eur T Electr Power 2003; 13: 47-54.